

A Chapter in Scaffolding in Tissue Engineering

PuraMatrix: Self-assembling Peptide Nanofiber Scaffolds

Shuguang Zhang^{*¶}, ^ΔRutledge Ellis-Behnke, Xiaojun Zhao[¶],
and [†]Lisa Spirio

[¶]Center for Biomedical Engineering, NE47-379,

^{*}Center for Bits & Atoms

^ΔDepartment of Brain and Cognitive Science

Massachusetts Institute of Technology

77 Massachusetts Avenue

Cambridge, MA 02139-4307

[†]3-DMatrix, Inc., Cambridge, MA, www.puramatrix.com

Tel.: 617-258-7514, FAX: 617-258-0204

Shuguang@mit.edu, <http://web.mit.edu/lms/www>

Table of Content

1. INTRODUCTION

1.1. Animal-derived ECM and synthetic scaffolds

1.2. PuraMatrix Peptide Nanofiber Scaffolds

Nanofiber-scale synthetic ECM

Defined 3-D microenvironments for cell biology

1.3 3-D Cell Culture Versus 2-D

1.4. Nanoscale Fibers Versus Microscale

1.5. Ideal synthetic biological scaffolds

2. SELF-ASSEMBLING PEPTIDES

2.1. Discovery and Development of Self-assembling Peptides.

Simple repeating units of amino acids assemble into nanofiber scaffolds

Amenable to design incorporating bioactive elements

2.2. Structural Properties of Self-assembling Peptides

3. PEPTIDE NANOFIBER SCAFFOLDS

3.1. EAK16-II

3.2. RADA16

3.3. KFE8 and KLD12

4. PURAMATRIX IN VITRO CELL CULTURE EXAMPLES.

4.1. Hepatocytes

4.2. Adult Liver Progenitor Cells

4.3. Chondrocytes Form Molded Cartilage in Cell Culture

4.4. Extensive Neurite Outgrowth and Active Synapse Formation on PuraMatrix

- 4.5. Organotypic Hippocampal Tissue Culture in PuraMatrix
 - 4.6. Murine Embryonic Stem Cells
 - 4.7. Osteoblasts
5. STANDARD IN VITRO TOXICOLOGY AND BIOCOMPATIBILITY STUDIES
- 5.1. Cytotoxicity
 - 5.2. Hemolysis
 - 5.3. Coagulation Prothrombin Time
6. IN VIVO BIOCOMPATIBILITY AND TOXICOLOGY STUDIES
- 6.1. ADME and Biodegradability
 - 6.2. Rabbit Muscle Implant (2 weeks)
 - 6.3. Peptide Nanofiber Scaffold for Brain Lesion Repair in Hamsters.
 - 6.4. Intracutaneous Reactivity
 - 6.5. Rabbit Pyrogen
7. FUTURE PERSPECTIVE
- 7.1. Forward-Compatible with Bioproduction and Clinical Applications.
 - 7.2. Synthetic Origin, Clinical-Grade Quality, Clinical Delivery.
 - 7.3. Tailor-made PuraMatrix
8. ACKNOWLEDGEMENTS
9. REFERENCES

1. INTRODUCTION

The fields of tissue engineering and reparative and regenerative medicine require two key complementary components: 1) a suitable biological scaffold that creates a microenvironment niche for a given cell type, and 2) that the given cell type can rapidly integrate and coalesce into the needed tissue.

The three-dimensional assembly of cells in a biological microenvironment is designed to recapitulate normal tissue function (1). Often this involves the use of biomaterials. The task of the biomedical engineering is to design and to select optimal biomaterials with the properties most closely matched to those needed for a particular application (2-6).

Stem cells and phenotypically plastic cells hold high hopes for tissue engineering, reparative and regenerative medicine. In most cases, these cells must be paired with microenvironments, which instruct proper expansion and/or differentiation, through mimicry of the native in vivo microenvironments and basement membranes and with a critical constituent being the extracellular matrix (ECM) (7-9). This fibrous protein scaffold not only provides the appropriate three-dimensional architecture, but also promotes signaling pathways influencing critical cell functions such as proliferation, differentiation, and migration (10-11). Moreover, the fields of tissue engineering, stem cell biology, and cancer biology are realizing that the ECM and a fine-tuned three-dimensional microenvironment are critical for the proper understanding and manufacturing of successful clinically-relevant therapies.

However, most cell biology research has used two-dimensional constructs to study single cell populations treated selectively with soluble factors in a homogeneous environment (12). This greatly simplifies the research models, but also mitigates the powerful effects of ECM and 3-D culture conditions on the cells of interest. Recreating 3-D conditions and structures in vitro, rather than growing cells in 2-D Petri dishes and flasks, have yielded tools for more accurate biological analyses (13, 14).

1.1. Animal-derived ECM and synthetic scaffolds

In the past two decades have witnessed the quest for synthetic biocompatible polymers, hydrogels, and or animal-derived materials (2-6). Until recently, 3-D cell culture has required either synthetic scaffolds, which fail to approximate the physical nanoscale size and chemical attributes of native ECM, or animal-derived materials, which may confound cell culture with undefined or inconsistent variables. Biomaterials such as PLLA and PGA biopolymers, calcium phosphate mesh, PEG gels, methylcellulose, alginates and agarose have seen limited success, partly due to either their large microfiber size relative to cells, acidic breakdown products, charge density, lower nutrient diffusion rates, or inability to allow the creation of functional microenvironments by the cells. Animal derived biomaterials including bovine collagen and gelatin, fibronectin, intestinal submucosa, cadaver tissue, and Matrigel may help to create the right microenvironments, but complicate research and therapies with their potential risk of other unknown material contaminations, thus rise issues about cell signaling, protein content, and reproducibility.

We have described a family of synthetic self-assembling peptide scaffolds (SAPS), which we now call PuraMatrix because of its synthetic nature and extreme purity of a single peptide component. PuraMatrix not only can be used as a coating or to encapsulate cells similar to the ECM, but can also be tailor-made for particular cells, tissues and therapies.

1.2. PuraMatrix Peptide Nanofiber Scaffolds

Over the past 10 years, a new class of biologically-inspired peptide biomaterials has been discovered and developed in the context of cell culture, stem cell biology and tissue engineering. These self-assembling peptide scaffolds have been used successfully as a synthetic *in vitro* and *in vivo* ECM, proving themselves as a critical component to successful 3-D cell growth.

Nanofiber-scale synthetic ECM

PuraMatrix is a 16 amino acid synthetic peptide that is resuspended in water to generate a range of solution concentrations. Upon the introduction of millimolar amounts of monovalent cations, either through the addition of salt solution, cell culture media or injection of the material *in vivo*, PuraMatrix undergoes self-assembly into nanofibers, ~10 nm in diameter, on a scale similar to the *in vivo* extracellular matrix (ECM). The physical size relative to cells and proteins, the amphiphilic peptides' charge density, and water-structuring abilities mimic the *in vivo* ECM. These well-ordered nanofibers create 3-dimensional porous scaffolds that are very difficult or impossible to synthetically produce by other manufacturing techniques. The nanofiber density and average pore size, ~5-200 nm, correlates with the concentration of peptide solution that is used to produce the material, which can be varied from 0.1 to 3% in water (1-30mg/ml w/v) depending on the application.

Defined 3-D microenvironments for cell biology

PuraMatrix mimics several important aspects of the *in vivo* environment – a synthetic ECM – enabling defined cell culture conditions while allowing cells to proliferate and differentiate within a 3-D context, easily migrate within that microenvironment, and create their own microenvironments quickly including production of their own ECM.

1.3. 3-D Cell Culture Versus 2-D

The advancement of biological study often requires the development of new materials, methods and tools. The introduction of the Petri dish over 100 years ago provided an indispensable tool for culturing cells *in vitro*, thus permitting the detailed dissection of seemingly intractable biology and physiology systems into manageable units and well-defined studies. This simple dish has had profound impact on our understanding of complex biology, especially cell biology and neurobiology.

However, the Petri dish culture system, including multi-well plates, glass cover slips, etc, is less than ideal for several reasons: 1) It is a 2-dimensional (2-D) system which is in sharp contrast to the 3-D environment of natural tissues both animal and plant. 2) The Petri dish surface without coating is rigid and inert, again in sharp contrast to the *in vivo*

environment where cells intimately interact with the extracellular matrix and with each other. 3) The tissue cell monolayers on coated 2-D surface, such as poly-L-lysine, collagen gels, fibronectin, and laminin as well as other synthetic materials containing segments of adhesion motifs, have only part of the cell surface attached to the materials and interact neighboring cells. The remaining parts are often directly exposed to the culture media, unlike the tissue environment where every cell intimately interact with its neighbors and the ECM. 4) The transport phenomena of 2-D and 3-D are drastically different. In 2-D culture systems, cytokines, chemokines and growth factors quickly diffuse in the media across the culture dish. This is again in sharp contrast to the in vivo environment where chemical and biological gradients play a vital role in signal transduction, chemotaxis, cell-cell communications and development. Cells respond to local concentrations of a variety of molecules, which in traditional cell culture, are distributed homogenously. Yet, most cells, by virtue of being embedded in a tissue, live in an environment that contains a dynamic gradient of nutrients and secreted factors – a “spatial heterogeneity” that cannot be emulated using conventional 2-d tissue culture. Since many cell types secrete their own ECM, a synthetic scaffold can be used even if not initially coated with the particular ECM proteins. 5) Cells cultured on a 2-D Petri dish are not readily transportable, and it is challenging to move cells from one environment to another without incurring changes in the cell-material and cell-cell interactions. For example, enzymatic cell harvesting using trypsin or mechanical disruption using rubber policeman both may have adverse effects on cell-environment interactions. Culturing to on 2-D surfaces to cell confluence requires frequent passages, including more reagent costs and cell manipulation. In contrast, cells cultured in 3-D are more readily transportable without significantly harming cell-material and cell-cell interactions, thus providing a significantly new way to study cell biology.

1.4. Nanoscale Fibers Versus Microscale

In the last two decades, several biopolymers, such as PLLA, PLGA, PLLA-PLGA copolymers and other biomaterials including alginate, agarose, collagen gels, etc, have been developed to culture cells in 3-D (2-6). These culture systems have significantly advanced our understanding of cell-material interactions and fostered a new field of tissue engineering. However, these biomaterials are often made of microfibers with diameters of 10-100 microns – drastically different in size, surface interaction, porosity, and concentration relative to the native ECM and cells interacting with it. Therefore, cells attached on microfibers are in fact, in 2-D despite the various curvatures associated with the large diameter microfibers. In order to culture cells in a truly 3-D microenvironment, the fibers must be significantly smaller than cells so that the cells are surrounded by the scaffold, similar to the extracellular environment and native ECM.

Size does make big difference

Trees, 20-30 cm in diameter

Grass, 0.5 cm in diameter



Swedish forest

Scotland

Fig. 1. Size does make a big difference. The trees shown on the left are 20-30 centimeters in diameter and the distance between the trees is in tens of meters. Animals can't walk through, the trees but can walk between them. On the other hand, grass is about 0.5 centimeter in diameter. When animals walk in the grass field, they are surrounded by the grass.

We believe that the development of new biological materials, particularly those biologically-inspired nanoscale scaffolds mimicking in vivo environment that serve as permissive substrates for cell growth, differentiation and biological function is a key area of study. These materials will be useful not only for further our understanding of cell biology in 3-D environment, but also for advancing medical technology, tissue engineering, regenerative biology and medicine.

1.5. Ideal synthetic biological scaffolds

The ideal biological scaffold and its building blocks should meet several criteria:

- 1). derived from chemically-defined, synthetic sources which are present in native tissue;
- 2). amenable to design and modification to customize specific bioactive and functional requirements;
- 3). allow cell attachment, migration, cell-cell, cell-substrate interactions, and recovery of cells from the scaffold;
- 4). exhibit no cytotoxicity or biocompatibility problems while chemically compatible with aqueous solutions, cell culture and physiological conditions
- 5). compatible with microscopy, molecular biology analysis, flow cytometry
- 6). sterile and stable enough for shelf life, transportation, bioproduction and closed system cell therapy culture

- 7). economically viable and scaleable material production, purification and processing;
- 8). exhibit a controlled rate of material biodegradation in vivo with nondetectable immune responses and inflammation;
- 9). foster cell migration and angiogenesis to rapidly integrate with tissues in the body.
- 10). injectable along with cells, compatible with cell delivery and surgical tools;

2. SELF-ASSEMBLING PEPTIDES

2.1. Discovery and Development of Self-assembling Peptides.

Simple repeating units of amino acids assemble into nanofiber scaffolds

The first molecule of this class of self-assembling peptides, EAK16-II, a 16 amino acid peptide, was found as a segment in a yeast protein, zuotin which was originally characterized by binding to left-handed Z-DNA (15). Zuotin is a 433-residue protein with a domain consisting of 34 amino acid residues (305-339) with alternating alanines and alternating charges of glutamates and lysines with an interesting regularity, AGARAEAEAKAKAEAEAKAKAESEAKANASAKAD (15). We subsequently reported a class of biological materials made from self-assembling peptides (16-22). This biological scaffold consists of greater than 99% water content (peptide content 1-10 mg/ml). They form scaffolds when the peptide solution is exposed to physiological media or salt solution (23-26).

The scaffolds consist of alternating amino acids that contain 50% charged residues (16-20, 23-27). These peptides are characterized by their periodic repeats of alternating ionic hydrophilic and hydrophobic amino acids. Thus, the β -sheets have distinct polar and non-polar surfaces (16-20). A number of additional self-assembling peptides including RAD16-I and RAD16-II, in which arginine and aspartate residues substitute lysine and glutamate have been designed and characterized for salt-facilitated scaffold formation (16-20). Stable macroscopic matrix structures have been fabricated through the spontaneous self-assembly of aqueous peptide solutions introduced into physiological salt-containing solutions. Several peptide scaffolds have been shown to support cell attachment of a variety of mammalian primary and tissue culture cells (16-22).

Amenable to design incorporating bioactive elements

Since these peptides are synthetic and molecular-engineered, they can be modified through the incorporation of particular active sequences for specific ECM-cell interactions. We have carried out successful experiments with a number of active sequences, as yet unpublished, with important implications for 3-D cell culture and tissue engineering (C. Semino, unpublished results).

2.2. Structural Properties of Self-assembling Peptides

In general, these self-assembling peptides form stable β -sheet structures in water. They are stable across a broad range of temperature, wide pH ranges in high concentration of denaturing agent urea and guanidium hydrochloride. Although sometimes, they may not form long nanofibers, their β -sheet structure remains largely unaffected (16-17).

One of the possible reasons is their unique structure. The alternating alanine residues in PuraMatrix are similar to silk fibroin such that the alanines can pack into inter-digital hydrophobic interactions. The ionic complementary sides have been classified into several moduli (modulus I, modulus II, modulus III, modulus IV, etc., and mixtures thereof). This classification scheme is based on the hydrophilic surface of the molecules that have alternating positively and negatively charged amino acids, alternating by 1 residue, 2 residues, 3 residues, and so on. For example, charge arrangements for modulus I, modulus II, modulus III, and modulus IV are $-+-+--+$, $--+ +--++$, $---+++$, and $----++++$, respectively. The charge orientation can also be designed in the reverse orientation, which can yield entirely different molecules. These well-defined sequences allow the peptides to undergo ordered self-assembly, resembling some situations found in well-studied polymer assemblies.

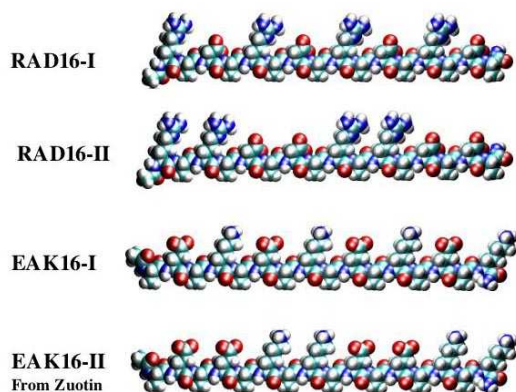


Fig. 2. Molecular models of several self-assembling peptides, RAD16-I, RAD16-II, EAK16-I and EAK16-II. Each molecule is ~5nm in length with 8 alanines on one side and 4 negative and 4 positive charge amino acids in an alternating arrangement on the other side.

3. PEPTIDE NANOFIBER SCAFFOLDS

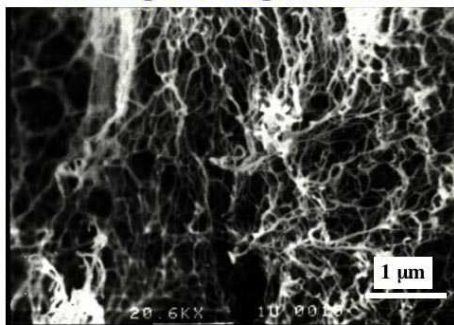
3.1. EAK16-II

The EAK16-II, AEA EAKAKAEAEAKAK, is the first member in the self-assembling peptide family. EAK16-II was the first peptide to be characterized in detail (16-18, 28) and has also been shown to retain β -sheet structure for extended periods of time (One sample was stable for over 10 years, Zhang, unpublished results). An EAK membrane-like scaffold was first discovered in the tissue culture media where PC12 cells were used to test for EAK16-II cytotoxicity. The EAK scaffold showed no apparent toxicity, but instead, the

PC12 cells were found to attach onto the membranous materials where EAK16-II was added and not in the dishes where EAK8, a single unit of AEAEAKAK, was used (16). The membranous material was examined under SEM to reveal a well-ordered nanofiber structure (Fig. 3). Later using AFM, the nanofiber structure was confirmed (29).

Self-assembling Peptide Nanofibers

Scanning EM Image, EKA16-II



Zhang, et al., *PNAS*, April, 1993

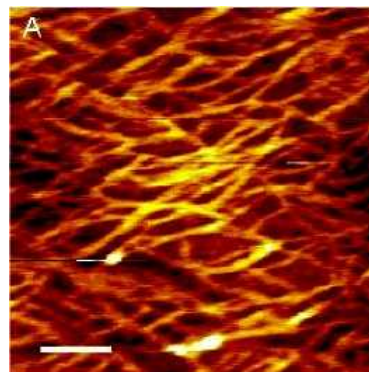


Fig. 3. EAK16-II nanofibers. EAK16-II nanofiber formation was demonstrated using SEM (16) and AFM (29). The nanofibers are ~10-20 in diameter with remarkable structural regularity. The scale bar in AFM is 200 nm.

3.2. RADA16

We then designed another several peptides altering the amino acid sequences containing RAD motif. RADA16-I, RADARADARADARADA, and RAD16-II, RARADADARADADADA, were studied (Fig. 2). These peptides have motif RAD that is similar to the ubiquitous integrin receptor binding site RGD. While it is not known if these RAD repeats in the Puramatrix scaffold behave similarly to RGD motifs, they have been studied in the context of cell attachment across a number of cell lines (18-19). These peptides form well-ordered nanofibers, similar as EAK16. Interestingly, RADARGDARADARGDA, and RADA8, RADARADA, did form stable β -sheet, nor nanofibers when studied under the identical conditions as RAD16. These observations suggest that the formation stable β -sheet is important not only for nanofiber but also for scaffold formation.

Furthermore, increasing concentration of RADA8 added into RAD16-I inhibited the long and well-ordered RADA16 nanofiber formation (Zhao, et al, unpublished results). Other variations of RAD16 including RAD16-IV and DAR16-IV have also been studied (30-33). DAR16 has an identical composition to RADA16-I but a different sequence arrangement. When it formed a β -sheet, the nanofibers are formed but upon heating, the DAR16 transformed into an α -helical structure and nanofibers were no longer observed (Zhao, et al., unpublished results). These results indicate that the most important factor for nanofiber formation is the structure rather than the composition or particular sequences used in the peptide.

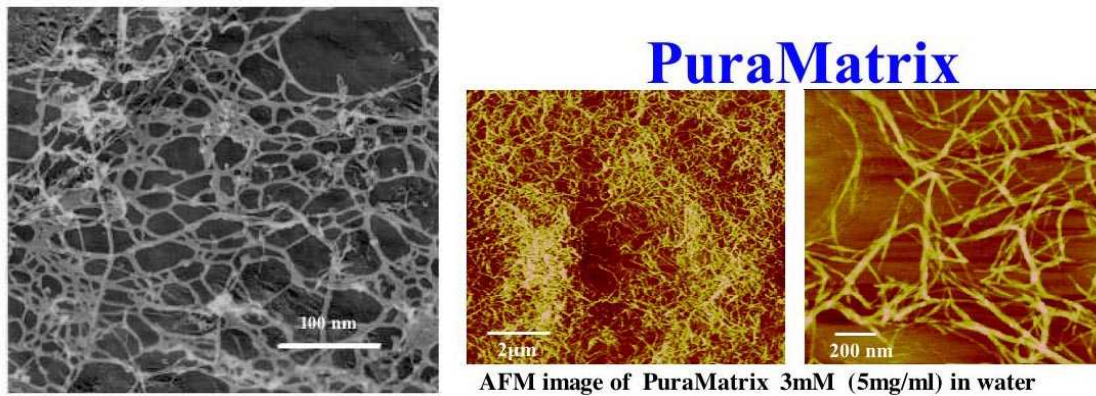


Fig. 4. PuraMatrix. A) TEM and B) AFM. Note the nanofiber scale fiber with pores ranging from 5-200 nm, the right pore size for biomolecular diffusion. This is in sharp contrast to the microfibrils of traditional polymer scaffolds, where the fiber diameter is ~1-50 micron and the pores range from 10-200 microns.

3.3. KFE8 and KLD12

Self-assembling peptides less than 16 residues have also been studied including KFE8 and KLD12 (Fig. 5) (20, 23-27, 34). Many self-assembling peptides that form scaffolds have been reported and the numbers are increasing (31-33). We now understand that the formation of the scaffold and its mechanical properties are influenced by several factors, one of which is the level of hydrophobicity (20, 23-27, 34). That is, in addition to the ionic complementary interactions, the extent of the hydrophobic residues, Ala, Val, Ile, Leu, Tyr, Phe, Trp (or single letter code, A, V, I, L, Y, P, W) can significantly influence the mechanical properties of the scaffolds and the speed of their self-assembly. The higher the content of hydrophobicity, the shorter the length required, the easier it is for scaffold formation and the better for their mechanical properties (20, 23-27, 34). Interestingly, different cells may behave differently in different peptide scaffolds depending on the culture conditions. This again demonstrates the importance of tailor-making scaffolds for different tissue cells microenvironment.

Mouse fibroblast	Bovine calf & adult chondrocytes
Chicken embryo fibroblast	Bovine endothelial cells
Chinese hamster ovary	Rat adult liver progenitor cells
Rat pheochromocytoma	Rat cardiac myocytes
Rat neural stem cells	Rat hippocampal neural tissue slice
Mouse embryonic stem cells	Mouse neural colony stem cells
Mouse cerebellum granule cells	Mouse & rat hippocampal cells
Bovine osteoblasts	Hamster pancreas cells
Human cervical carcinoma	Human osteosarcoma
Human hepato-cellular carcinoma	Human neuroblastoma
Human embryonic Kidney	Human foreskin fibroblast
Human epidermal keratinocytes	Human neural stem cells

These cells include stable cell lines, primary isolated cells from animals, progenitor and stem cells.

4.1. Hepatocytes

Hepatocytes have been cultured on PuraMatrix and Matrigel where they attach, proliferate, exhibited proper spheroid morphology and created tight junctions. On the other hand, hepatocytes cultured on collagen coated Petri dish did not survive for long term, and didn't attach when cultured on plastic dish alone.

Hepatocyte morphology was evaluated at day 2 and day 5. Cytochrome p450 1A1 was evaluated as follows on day 10. Substrate 8 μ M 7-ethoxyresorufin metabolized by cells for 30 minutes at 37°C to resorufin conjugate. Fluorescence was measured at 530 nm excitation and 590 nm emission. Acceptance criteria requires hepatocytes cultured on the Matrigel substrate is twice the level of hepatocytes on the collagen I substrate. Hepatocytes on PuraMatrix grew much better than collagen I thus suggesting PuraMatrix is a suitable scaffold for hepatocytes culture in vitro.

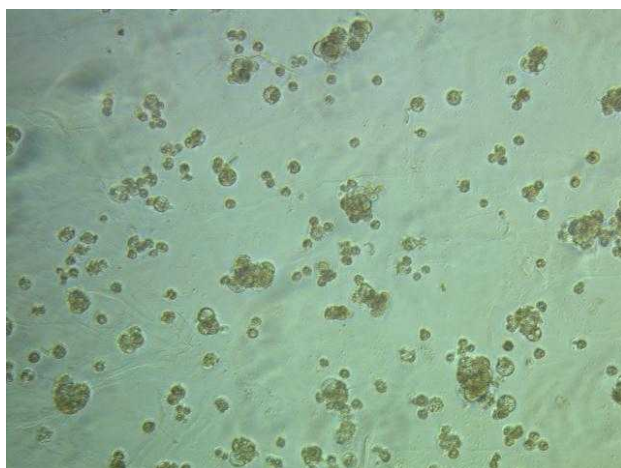


Figure 6. Primary rat hepatocytes cultured on PuraMatrix at Day 5. Cells begin to form clusters.

4.2. Adult Liver Progenitor Cells

A hepatocyte progenitor cell line has also been cultured using 3-D PuraMatrix. These cells exhibited non-exponential cell kinetics, acquired spheroidal morphology, and produces progeny cells with mature hepatocyte properties (21). The differentiated progeny cells display increased expression of albumin and several other indicators of hepatocyte maturation, including binucleation, up-regulation of transcription factor C/EBP α , and expression of cytochrome P450's CYP1A1, CYP1A2, and CYP2E1 (Fig. 7). In contrast, markers of hepatocyte progenitors, α -fetoprotein and CK8, are unchanged. These relationships suggest production of transition spheroidal units comprised of asymmetrically cycling adult progenitor cells and their differentiating progeny. All three cytochrome p450 enzyme activities are 3-methylcholanthrene-inducible in such spheroids. These results demonstrated the ability of a designed biological scaffold to provide a microenvironment in which adult progenitor cells regain their intrinsic ability to continuously produce differentiating progeny cells. This 3-D nanofiber scaffold may provide a physiological approach for biomedical applications and pharmaceutical high throughput drug screening tools with more reliable content outcome (21).

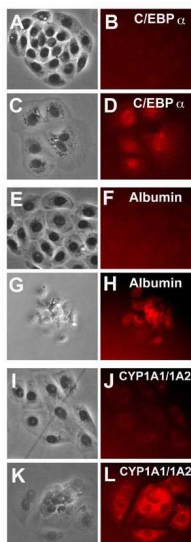


Figure 7. Promotion of hepatocyte differentiation by PuraMatrix. Lig-8 hepatic progenitor cells were cultured in 2-D adherent culture or in 3-D PuraMatrix. Spheroids were isolated and analyzed approximately 16 hours after transfer to adherent culture. **A, E, I**, adherent cell colonies (phase contrast); **B, F, J**, respective in situ immunofluorescence for adherent colonies with anti-C/EBP α , anti-albumin, and anti-CYP1A1/1A2 antibodies; **C, G, K**, isolated scaffold spheroids (phase contrast; note binucleated cells); **D, H, L**, respective in situ immunofluorescence for isolated scaffold spheroids with anti-C/EBP α , anti-albumin, and anti-CYP1A1/1A2 antibodies.

4.3 Chondrocytes Form Molded Cartilage in Cell Culture.

In choosing a scaffold for cartilage repair, it is important to identify a material that can maintain a normal rate of proliferation of differentiated chondrocytes and a high rate of chondrocyte synthesis of specific ECM macromolecules including type II collagen and

GAGs until repair evolves into a steady-state tissue maintenance. Kisiday et al first used RADA16 scaffold but it did not give the optimal results because it is mechanically rather weak. We then designed the KLD12 (n-KLDLKLDLKLDL-c) peptide scaffold reasoning that as leucine is more hydrophobic than alanine, the leucines would likely pack more tightly in the nanofibers in aqueous conditions and thus provide a higher mechanical strength (20, 25-26).

Kisiday et al then used the self-assembling peptide KLD12 scaffold as a model for cartilage repair and developed a method to encapsulate chondrocytes within the scaffold. During 4 weeks of culture in vitro, chondrocytes seeded within the peptide scaffold developed a cartilage-like extracellular matrix (ECM) rich in proteoglycans and type II collagen, indicative of a stable chondrocyte phenotype. Time dependent accumulation of this ECM was paralleled by increases in material stiffness indicative of deposition of mechanically functional newly formed tissue. The content of viable differentiated chondrocytes within the peptide scaffold increased at a rate that was 4-fold higher than that in parallel chondrocyte-seeded agarose culture, a well-defined reference chondrocyte culture system. These results demonstrate the potential of a tailor-made peptide scaffold as a scaffold for the synthesis and accumulation of a true cartilage-like ECM in a 3-D cell culture for cartilage tissue repair. The peptide KLD12 used in this study represents a designed self-assembling peptide made through molecular engineering that can be modified to suit specific cell and tissue application interests (20).

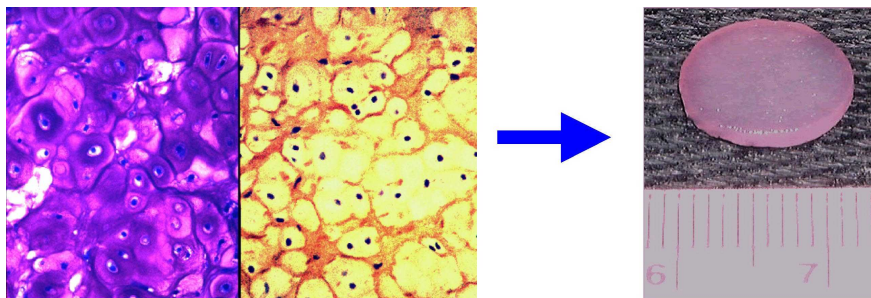


Figure 8. Peptide KLD12 (KLDLKLDLKLDL), chondrocytes in the peptide scaffold and cartilage. **A)** The chondrocytes stained with TB showing abundant GAG production (left panel) and antibody to type II collagen demonstrating abundant Type II collagen production (right panel). **B)** A piece of pre-molded cartilage with encapsulated chondrocytes in the peptide nanofiber scaffold. The cartilage formed over a 3-4 week period after the initial seeding of the chondrocytes (20).

4.4. Extensive Neurite Outgrowth and Active Synapse Formation on PuraMatrix

PuraMatrix serves as a substrate and portable membrane media to support both neuronal attachment and differentiation in the form of extensive neurite outgrowth. Functional synapse formation also occurs between attached neurons when the cells are grown on PuraMatrix (19). Neurite outgrowth from primary neuronal cultures was also tested by using several nerve cell types, including primary dissociated neurons from the mouse cerebellum and rat hippocampus. Cerebellar granule neurons undergo postnatal development and are morphologically distinguishable from other cerebellar cells. PuraMatrix scaffolds support extensive neurite outgrowth from cerebellar granule neurons prepared from 7-day-old mice and the neurites were

readily visualized in two different focal planes, suggesting that the neurites closely follow the contours of the matrices. The primary cerebellar neuronal cultures on the PuraMatrix scaffolds were maintained for up to 4 weeks. Dissociated mouse and rat hippocampal neurons also attach and project neurites on the scaffolds (Table 2).

Table 2. Neurite outgrowth on PuraMatrix membrane surface.

Cell type	length of process (micron)	Cell sources
NGF-treated Rat PC12	400–500	Cultured cell line
NGF-preprimed PC12	400–500	Cultured cell line
Human SY5Y neuroblastoma	400–500	Cultured cell line
Mouse cerebellar granule neurons	200–300	‡ Primary cells
Mouse hippocampal neurons	100–200	‡ Primary cells
Rat hippocampal neurons	200–300	§ Primary cells

ells were seeded onto PuraMatrix scaffold coating. The cell-bearing PuraMatrix was transferred to dishes with fresh medium. Maximum neurite length was estimated visually with scale bars 3–7 days after cell attachment for primary cultures and 10–14 days after matrix attachment for the cultured cell lines. ‡Seven-day-old mouse. §One-day-old rat.

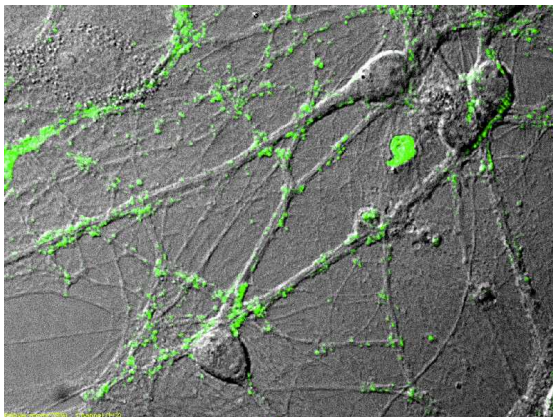


Figure 9. Active synapses on the peptide surface. Primary rat hippocampal neurons form active synapses on peptide scaffolds. The confocal images shown bright discrete green dot labeling indicative of synaptically active membranes after incubation of neurons with the fluorescent lipophilic probe FM-143. FM-143 can selectively trace synaptic vesicle turnover during the process of synaptic transmission. The active synapses on the peptide scaffold are fully functional, indicating that the PuraMatrix is a permissible substrate for neurite outgrowth and active synapse formation (19).

4.5. Organotypic Hippocampal Tissue Culture in PuraMatrix

PuraMatrix has also been used to isolate and expand self-renewing neural cells ex vivo. Neurogenesis occurs in restricted areas of postnatal mammalian brain including the dentate gyrus and subventricular zone (SVZ). (22). PuraMatrix has been used to entrap migrating neural cells (potential neuroprogenitors) from postnatal hippocampal

organotypic cultures in 3-D PuraMatrix. In those experiments, brain tissues from the rat neonatal hippocampus were laid on top of preformed PuraMatrix and cultured for up to 2 weeks. Within a few hours, cell division activity was observed only at the interface zone (22). The migrating neural cells with mitotic activity from the dentate gyrus, CA1, CA2, and CA3 regions of the post-natal rat hippocampus were greatly enriched in organotypic culture and entrapped them in PuraMatrix. After a few hours, the cells exhibited high proliferating activity as measured by incorporation of BrdU⁺ cells at the “interface zone” between the tissue slice and the culture surface. Using PuraMatrix for neural progenitor cell isolation and expansion in vitro may thus have applications in developing new strategies and for cell-based therapies in regenerative medicine.

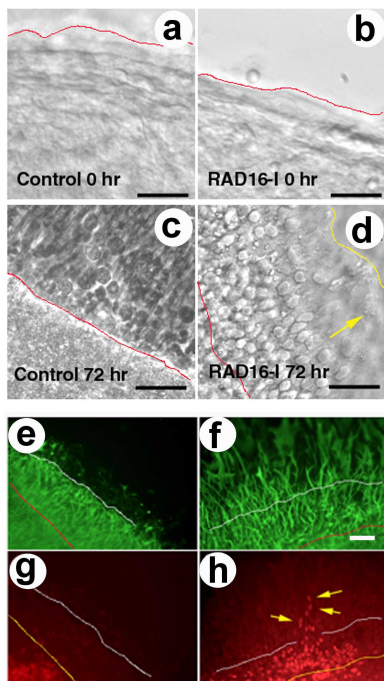


Figure 10. Hippocampal organotypic slice cultures cultured on peptide scaffolds develop extended tissue scaffolds (22). Hippocampal slices were cultured organotypically either on control membrane or on RAD16-I peptide scaffolds layers (~500 μm thick). Time laps experiment was carried out to follow up the tissue scaffold growth from the perimeter of the dentate gyrus region. **a)** time 0 (0 hr) of control slice culture; **b)** time 0 (0 hr) of scaffold slice culture; **c)** 72 hrs of control slice culture; **d)** 72 hrs of scaffold slice culture. The red line indicates the original border of the tissue slice and the yellow in **d)** the extended tissue scaffold. The yellow arrow in **d)** indicates the direction of tissue scaffold growth and extension. Black bars indicate 100 μm . **e)** 72 hrs control slice culture immunostained for GFAP (glia cell marker, green); **f)** 72 hrs scaffold slice culture immunostained for GFAP (green); **g)** same optical layer as **e)** immunostained for NeuN (neuron marker, red); **h)** same optical layer as **f)** immunostained for NeuN (red). Red lines in **e)** and **f)** and yellow in **g)** and **h)** indicates the original perimeter of the tissue slice. The white line in **e)** and **g)** indicates the extended tissue scaffold in the control cultures. The white line in **f)** and **h)** is use to compare the over extension obtained on peptide scaffolds cultures. Yellow arrows in **h)** indicate neuron cells staining with NeuN (red) migrating into scaffold slice cultures. The white bar in **f)** is 100 μm .

4.6. Murine Embryonic Stem Cells

Embryonic stem cells represent an important tool not only for the study of developing tissues and organisms, but also in the goal to providing more effective cell therapies. In order to grow embryonic stem cells in a clinically-compatible manner, mouse and human ES cells were tested on PuraMatrix. In the absence of feeder layers, 35 passages of murine embryonic stem cells have obtained when cultured in 3-D PuraMatrix and maintained in an undifferentiated state (B. Lahn, unpublished results). These mouse ES cultures continue to express both the Oct-4 and SSEA-1 markers for undifferentiated ES cells and the cells are currently being tested for germline transmission in the mouse (B. Lahn, unpublished results). Additionally, the human ES cell line, H9, was maintained for one week in an undifferentiated state on PuraMatrix. The H9 cells grown on PuraMatrix were equally undifferentiated compared to H9 cells grown on Matrigel/conditioned media cocktails. An ES cell marker, tra 160, (human ES cell differentiation) and flow cytometry analysis were used to confirm the ES cell state (L. Daheron & G. Daley, unpublished results). Taken together, these preliminary results suggest that PuraMatrix is very promising to be useful in maintaining undifferentiated ES cells.



Fig. 11. Murine embryonic stem cells in PuraMatrix (Image courtesy of 3-DMatrix). Note the cell cluster formation, a characteristic of ES cells.

4.7. Osteoblasts

Osteoblasts (ATCC MT3T3) have been maintained with increase cell density successfully in PuraMatrix up to one month (3-DMatrix, unpublished results). These cells not only proliferated but also formed gap junctions connecting osteoblasts in a manner that is also found in native bone tissues.

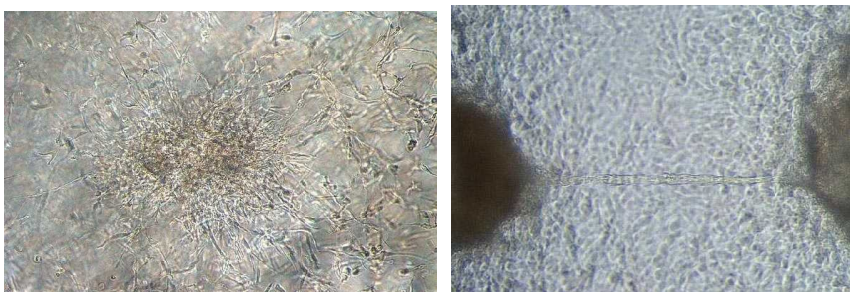


Fig. 12. Osteoblasts in PuraMatrix. Cells form clusters (left panel) and junctions connected by cells (right panel) (Image courtesy of 3-DMatrix).

5. STANDARD IN VITRO TOXICOLOGY AND BIOCOMPATIBILITY STUDIES

In addition to over 8 years of cell culture studies in our laboratory and elsewhere, standard in vitro toxicology studies have been completed, including EN/ISO tests for cytotoxicity and hemocompatibility. The tests below were completed at a FDA certified toxicology testing company (Toxikon Corp, Bedford, MA) using established standards of measure on the commercially-available PuraMatrix (RADI-16) (Table 3).

Table 3. In vivo biocompatibility and toxicology tests.

TEST	*RESULT
Cytotoxicity:	
Agar Diffusion ISO 10993-5	Non-cytotoxic
Hemolysis:	
Direct Contact (ISO 10993-4)	Non-hemolytic
Prothrombin Time Assay:	
Human Plasma (ISO 10993-4)	No adverse effect on prothrombin coagulation

*These tests are contract to the FDA certified commercial toxicology test facility (Toxikon Corp, Bedford, MA.).

5.1. Cytotoxicity

The Agar Diffusion test (ISO 10993-5) measures a material's effect on cell cultures, which are extremely sensitive to minute quantities of leachable chemicals and readily display characteristic signs of toxicity in the presence of potentially harmful leachables. The biological reactivity of a mammalian monolayer, L929 mouse fibroblast cell culture, in response to the test article was determined as "no-reactivity" in tests.

5.2. Hemolysis

The hemolysis test (Direct Contact, ISO-10993-4) measures the ability of a material to cause red blood cells to rupture. This test is derived from well-established NIH protocols and is performed in triplicate. This test uses rabbit blood in direct contact with the test material and the degree of hemolysis is measured spectrophotometrically. PuraMatrix tested "non-hemolytic" in tests carried out by an independent FDA-certified testing agency.

5.3. Coagulation Prothrombin Time

Prothrombin Time (Human Plasma, ISO 10993-4) measures the effect of a test article extract on human blood coagulation time. This assay has become a suitable clinical means of determining the presence and functioning ability of prothrombin in the process of coagulation. PuraMatrix did not have an adverse effect on prothrombin coagulation time of human plasma, in tests carried out by an independent FDA-certified testing agency.

6. IN VIVO BIOCOMPATIBILITY AND TOXICOLOGY STUDIES

Several kinds of biocompatibility and toxicity examinations of PuraMatrix RAD have been carried out in numerous animal models, including a number of standard FDA/ISO toxicology and in vivo implant studies, to assess the safety of PuraMatrix. PuraMatrix has passed each and every one. These tests point to the biocompatibility of this particular peptide material, but more long-term studies are required to complete on the way to commercialization for therapeutic applications (Table 4). These tests were conducted on a fee for service basis under GLP conditions by Toxikon Corporation, an FDA-certified facility in Bedford, Mass.

Moreover, previously studies of animal reactions (19, 35) described lack of immunogenicity and inflammation in rat, rabbit, goat, and hamster models.

Table 4. PuraMatrix used in vivo animal studies

TEST	*RESULT
ADME Tox: 14 day implant	No problematic organ accumulation, excretion. ¹⁴ C Radiolabeled PuraMatrix 10% excreted by day 14
Rabbit Muscle Implant: 14 day (ISO 10993-6)	Non-toxic score across 13 categories of reactions
Rabbit Pyrogenicity: 24 hour (ISO-10993-11)	No effect on animals
Intracutaneous Implant: 72 hours (ISO 10993-12)	Primary Irritation Index = 0.0 “Negligible” No febrile reaction from any animal over 24 hours after intravenous injection of dilute solution.
CNS Lesions in Hamsters: 2-60 days	Reduced scarring and reinnervation across the severed optic tract caudal to the lesion only in PuraMatrix-treated animals (35)

6.1. ADME and Biodegradability

In order to measure the local and whole animal distribution of PuraMatrix, and given that previous experiments were unable to raise antibodies to it, we generated a ¹⁴C, carbon radiolabeled version of PuraMatrix. The radiolabeled version was internally labeled at the third alanine site (Acetyl-(RADA)-(R-[¹⁴C(U)-Ala]-D-A)-(RADA)₂-CONH₂) as opposed to a labeled acetyl group which could be cleaved off, in order to better characterize the adsorption, degradation, metabolism and excretion (ADME) of the PuraMatrix material in vivo.

The radiolabeled PuraMatrix was then implanted into Sprague Dawley rats in a femur defect model. Urine and stool samples were collected and the radioactivity was counted.

6.2. Rabbit Muscle Implant (2 weeks)

This test assesses the local effects of material on contact with living tissue. Test article was implanted into paravertebral muscle of 3 New Zealand white rabbits, with negative control (GelFoam) implanted in the contralateral muscle of each animal. Healing was allowed for 2 weeks. Animals were sacrificed and implants excised. Excised implants were examined macroscopically with a magnifying lens and fixed in formalin. Histologic slides of hematoxylin and eosin (H&E) and Mason's Trichrome stained sections were prepared, studied microscopically by a board-certified veterinary pathologist, and evaluated on a scale of 0-3.

PuraMatrix implants retained the initial implant volume, collagen fibers, and vascularization of the injection site. PuraMatrix was rated Non-Toxic (0.13) on a scale ranging from Nontoxic (<1), Slightly Toxic (1 to <2), Mildly Toxic (2 to <3), Moderately Toxic (3 to >4), to Severely Toxic (>4), in tests carried out by an independent FDA-certified testing agency.

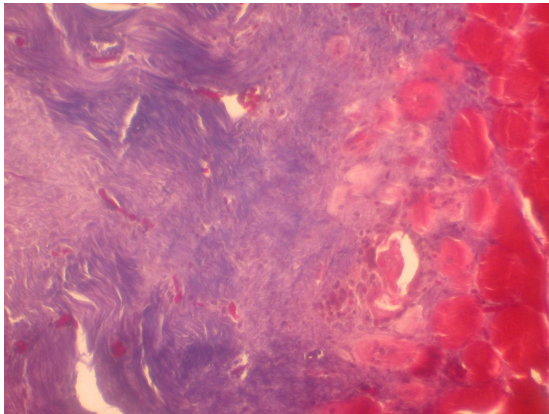


Figure 11. PuraMatrix creates a permissive environment for tissue bulking (two weeks post injection).

6.3. Peptide Nanofiber Scaffold for Brain Lesion Repair in Hamsters.

In another preliminary study, we used the RADA16 scaffold for brain lesion repair in Syrian hamsters. The nanofiber scaffold density correlates with the concentration of peptide solution and they retain extremely high hydration, >99% is water (5-10 mg/ml, w/v). In Vivo application to brain wounds was carried out using postnatal day-2 Syrian hamster pups that were anesthetized with whole-body cooling. The scalp was opened and the skull over the midbrain tectum was opened. The optic tract within the superior colliculus (SC) was completely severed with a deep knife wound, extending at least 1 mm below the surface, from the midline to a point beyond the lateral margin of SC. Animals were sacrificed at 1, 3, 6, 30 and 60 days for examinations. At surgery, 10 animals were treated by injection into the wound of 10 μ l of 1% RADA16. Control animals with the same brain lesion included 3 with isotonic saline injection (10 μ l), and numerous additional cases, including 10 in which the dye Congo red was added into the peptide scaffold, and 27 earlier animals with knife cuts and no injection surviving 6-9 days.

Histological specimen examinations revealed that only in the peptide scaffold-injected animals, but not in untreated animals, the brain tissue appears to have reconnected itself together in all survival times. Additionally, axons labeled from their retinal origin with a tracer molecule were found to have grown beyond the tissue bridge, reinnervating the SC caudal to the lesion (Fig. 9). Our preliminary experiments show it is possible to overcome a major barrier to functional CNS regeneration (Ellis-Behnke, et al., 2003).

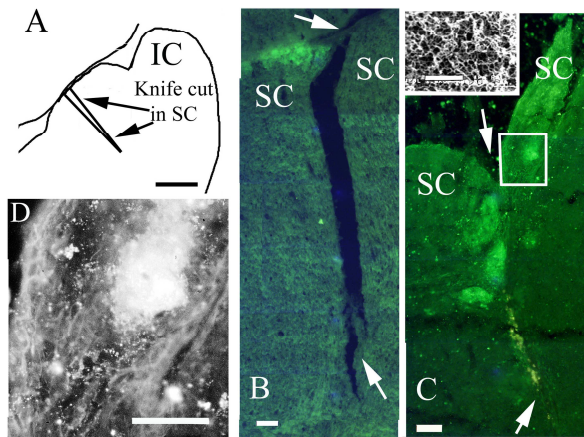


Figure 12. **A)** Schematic illustration of a parasagittal section of the dorsal midbrain of a hamster, with the position and depth of the surgical knife cut indicated. **B)** Parasagittal section from brain of 1-mo old hamster with saline-injected lesion at P2. The cavity shows the failure of the tissue to form a bridge over the lesion. Arrows: path of knife cut. **C)** Similar part of a section from a 1-mo hamster which had a P2 lesion injected with 10 μ l of 1% SAP RAD16-I. Retinal projections shown in green. Inset) The SAP scaffold seen in much higher magnification (scale bar 1 micron), taken with scanning electron microscope. **D)** Enlarged view of area indicated with the box in **C**; the re-grown axons, traced with a standard cholera-toxin fragment B labeling procedure using immuno-histochemistry, are seen in white; the bright region in the upper right is an area of dense termination seen with fluorescence microscopy. Scale bars: 500 microns in **A**; 100 microns in **B**, **C**, **D** except inset.

6.4. Intracutaneous Reactivity

Irritation reactivity tests assess the localized reaction of tissues, including breached tissue and blood contact, to device materials or extracts. A 0.5% w/v peptide PuraMatrix solution was extracted in NaCl and CSO at a ratio of 0.2gm per 1.0 mL at $70\pm 2^\circ\text{C}$ for 24 hours. Control extracts were prepared, in a similar manner to the test article. Three rabbits were injected intracutaneously, using one side of the animal for the test article extracts and the other side for the control extracts, at 0.2 mL per site. The injected sites were examined at 24, 48, and 72 hours post inoculation for gross evidence of tissue reaction such as erythema, edema, and necrosis. A Primary Irritation Index of 0.5 or less will be considered a negligible irritant, where 0.5 to <2 are slight irritants, 2 to <5 are moderate irritants, and >5 are severe irritants. The test sites injected with PuraMatrix did not exhibit any signs of erythema or edema through the 72 hour observation point. The Primary Irritation Index for the material is 0.0, in tests carried out by an independent FDA-certified testing agency.

6.5. Rabbit Pyrogen

The purpose of the test was to detect the risk of a patient to a febrile reaction as a result of the administration of the test article extract. The test article was prepared by mixing 9ml of the test article with 9mL of 0.9% USP Sodium Chloride for Injection (NaCl) and the resulting gel extracted at a ration of 0.2gm per 1.0 mL. The test article extract was administered by intravenous injection at 10 mL/kg. The rectal temperatures of the injected rabbits were compared with the temperature of a control rabbit similarly injected with 0.9% USP Sodium Chloride for Injection (NaCl). The base-line temperatures of the rabbits, determined no more than 30 minutes prior to injection of the test article extract, were used to exclude rabbits whose body temperatures vary by more than 1°C from each other and whose temperatures are greater than 39.8°C. Body temperatures were recorded at 30 minute intervals between 1 and 3 hours subsequent to injection. If no rabbit exhibited a rise in temperature of 0.5°C or more about its base-line temperature, the product met the requirements for the absence of pyrogens. None of the animals injected with the test article extract exhibited signs of pyrogenic response, in tests carried out by an independent FDA-certified testing agency.

7. FUTURE PERSPECTIVE

7.1. Forward-Compatible with Bioproduction and Clinical Applications.

PuraMatrix fulfills the best of both traditional biomaterials and a nanoporous/nanofiber gel to enable proper 3D cell growth and the creation of microenvironments surrounding cell colonies. For cells that prefer culture on a 2-D surface, we have experienced better results by culturing cells on PuraMatrix floating sheets, allowing a 3-D nutrient bath within the 2-D growth context.

PuraMatrix mimics important aspects of the in vivo environment, while eliminating complicating variables traditionally experienced from animal-derived materials. Unlike most other scaffolds, PuraMatrix can be sterilized through UV radiation or filtration, and has proven itself shelf-stable at room temperature for over 5 years. Not only lowering the handling, processing, transportation, and inventory costs, but also meeting the stringent bioproduction requirements through its synthetic composition, free of the signaling motifs and adventitious agents in animal product. PuraMatrix not only provides the 3-D context for cell research, but they are forward-compatible with bioproduction and clinical requirements necessary for eventual stem cell and tissue engineering therapies.

7.2. Synthetic Origin, Clinical-Grade Quality, Clinical Delivery

PuraMatrix is synthetic and sterile, hence suitable for bioproduction and can be readily used in bioproduction and clinical settings, unlike many animal derived materials (bovine or otherwise) that lack the consistent quality control, thus complicating clinical reproducibility and risking the introduction of undesirable contaminants (cell signaling motifs, prions, adventitious agents, etc.). PuraMatrix is currently manufactured in large scale quantities, some under GMP-grade processes and commercially available. Additionally, PuraMatrix can be used for closed, sterile system culture in vitro and can

also be injected in vivo without causing the immunoresponsive events that materials such as collagens and alginates can illicit. Upon injection or pipetting into solution, the PuraMatrix volume does not swell, retaining a consistent volume.

7.3. Tailor-made PuraMatrix

In order to fabricate tailor-made PuraMatrix, it is crucial to understand the finest detail of peptide and protein structures, their influence on the nanofiber structural formation and stability. Since there is a vast array of possibilities to form countless structures, a firm understanding of all available amino acids, their properties, the peptide and protein secondary structures is an absolute prerequisite for further advance fabrication of peptide and protein materials (36-37). We are moving in that direction and will further accelerate new scaffold development (38-40).

PuraMatrix so far used in diverse cell and tissue systems from a variety of sources demonstrated a promising prospect in further improvement for specific needs since tissues are known to reside in different microenvironments. The PuraMatrix used thus far are general peptide nanofiber scaffolds and not tailor-made for specific tissue environment. We are designing 2nd generation PuraMatrix scaffolds and to show that these tailor-made PuraMatrix incorporating specific functional motifs will perform as superior scaffolds in specific applications. They may not only create a fine-tuned microenvironment for 3-D tissue cell cultures, but also may enhance cell-materials interactions, cell proliferation, migration, differentiation and performing their biological function. The ultimate goal is to produce tailor-made scaffolds for particular tissue engineering, regenerative and reparative medical therapies.

Acknowledgement

We also would like to thank members of our lab, past and present, for making discoveries and conducting exciting research. We gratefully acknowledge the supports by grants from the US Army Research Office, Office of Naval Research, Defense Advanced Research Project Agency (BioComputing), DARPA/Naval Research Labs, DARPA/AFO, NSF-MIT BPEC and NSF CCR-0122419 to MIT Media Lab's Center for Bits & Atoms, National Institute of Health, the Whitaker Foundation, Du Pont-MIT Alliance, and Menicon, Ltd, Japan. We also acknowledge the Intel Corp., educational donation of computing cluster to the Center for Biomedical Engineering at MIT.

REFERENCES

1. J Sipe, Tissue Engineering and Reparative Medicine. Ann. N.Y. Acad. Sci. 961:1-9, 2002.
2. B Ratner, A Hoffman, F Schoen, J Lemons, (eds.) Biomaterials Science. Academic Press, New York. 1996.
3. R Lanza, R Langer, J Vacanti, Principles of Tissue Engineering, 2nd Academic Press, San Diego, CA. USA. 2000.
4. A Atala, R Lanza, Methods of Tissue Engineering. Academic Press, San Diego, CA. 2001.

5. AS Hoffman, Hydrogels for biomedical applications. *Advanced Drug Delivery Reviews*. 43: 3-12. 2002.
6. B Palsson, J Hubbell, R Plonsey, JD Bronzino, *Tissue Engineering: Principles and Applications in Engineering*. CRC Press, 2003.
7. S Ayad, RP Boot-Handford, MJ Humphreise, KE Kadler, CA Shuttleworth, *The extracellulat matrix: Facts Book*. 2nd, Academic Press, San Diego, CA. 1998.
8. T Kreis, R Vale, *Guide book to the extracellular matrix, anchor, and adhesion proteins*. 2nd., Oxford University Press. Oxford, UK, 1999.
9. Yannas, I. *Tissue and Organ Regeneration in Adults*. Springer, New York, 2001.
10. DJ Mooney, LK Hansen, R Langer, JP Vacanti, DE Ingber. Extracellular matrix controls tubulin monomer levels in hepatocytes by regulating protein turnover. *Mol Biol Cell*. 5:1281-1288, 1994.
11. P Friedl, K Zanker, E Brocker, *Cell migration strategies in 3-D extracellular matrix: Differences in morphology, cell matrix adhesions, and integrin function*. *Microscopy Research and Technique*. 43: 369-378, 1998.
12. A Folch, M Toner, *Microengineering of Cellular Interactions*. *Ann. Rev. Biomed. Eng.* 2: 227-256, 2000.
13. B Geiger, *Cell biology, Encounters in Space*. *Science* 294: 1708-1712, 2001.
14. A Abbott, D Cyranoski, *Biology's new dimensions*. *Nature* 420: 870-872, 2003.
15. S Zhang, C Lockshin, A Herbert, E Winter, A Rich (1992) Zuotin, a putative Z-DNA binding protein in *Saccharomyces cerevisiae*. *EMBO. J*, 11: 3787-3796.
16. S Zhang, T Holmes, C Lockshin, A Rich, Spontaneous assembly of a self-complementary oligopeptide to form a stable macroscopic membrane. *Proc. Natl. Acad. Sci. USA* 90: 3334-3338, 1993.
17. S Zhang, C Lockshin, R Cook, A Rich, Unusually stable beta-sheet formation of an ionic self-complementary oligopeptide. *Biopolymers* 34: 663-672, 1994.
18. S Zhang, T Holmes, M DiPersio, RO Hynes, X Su, A Rich, Self-complementary oligopeptide matrices support mammalian cell attachment. *Biomaterials* 16: 1385-1393, 1995.
19. TC Holmes, S Delacalle, X Su, A Rich, S Zhang, Extensive neurite outgrowth and active neuronal synapses on peptide scaffolds. *Proc. Natl. Acad. Sci. USA* 97: 6728-6733, 2000.
20. J Kisiday, M Jin, B Kurz, H Hung, CE Semino, S Zhang, AJ Grodzinsky, Self-assembling peptide hydrogel fosters chondrocyte extracellular matrix production and cell division: implications for cartilage tissue repair. *Proc. Natl. Acad. Sci. USA* 99: 9996-10001, 2002.
21. CE Semino, JR Merok, G Crane, G Panagiotakos, S Zhang, Functional differentiation of hepatocyte-like spheroid structures from putative liver progenitor cells in three-dimensional peptide scaffolds. *Differentiation* 71: 262-270, 2003.
22. CE Semino, J Kasahara, Y Hayashi, S Zhang, Entrapment of hippocampal neural cells in self-assembling peptide scaffold. *Tissue Engineering* 10: (in press) 2004.
23. EJ León, N Verma, S Zhang, DA Lauffenburger, RD Kamm, Mechanical properties of a self-assembling oligopeptide matrix. *J. Biomaterials Science: Polymer Edition* 9: 297-312, 1998.
24. M Caplan, P Moore, S Zhang, RD Kamm, DA Lauffenburger, Self-assembly of a

- beta-sheet oligopeptide is governed by electrostatic repulsion. *Biomacromolecules* 1: 627-631, 2000.
25. M Caplan, EM Schwartzfarb, S Zhang, RD Kamm, D Lauffenburger, Control of self-assembling oligopeptide matrix formation through systematic variation of amino acid sequence. *Biomaterials* 23: 219-227, 2002.
 26. MR Caplan, EM Schwartzfarb, S Zhang, RD Kamm, DA Lauffenburger, Effects of systematic variation of amino acid sequence on the mechanical properties of a self-assembling, oligopeptide biomaterial. *J. Biomaterials Science Polymer Edition* 13: 225-236, 2002.
 27. D Marini, W Hwang, DA Lauffenburger, S Zhang, RD Kamm Left-handed helical ribbon intermediates in the self-assembly of a beta-sheet peptide. *NanoLetters* 2: 295-299, 2002.
 28. S Zhang, Design and exploitation of self-assembling ionic complementary peptide systems: A model for peptide biomaterial engineering. *Perspective in Protein Engineering 1996 (CDROM Edition)* Geisow, M. Ed. Biodigm Ltd. UK, ISBN0-9529015-0-1, 1996.
 29. Y Hong, RL Legge, S Zhang, P Chen, Effect of amino acid sequence and pH on nanofiber formation of self-assembling peptides EAK16-II and EAK16-IV. *Biomacromolecules* 4: 1433-42, 2003.
 30. M Altman, P Lee, A Rich, S Zhang, Conformational behavior of ionic self-complementary peptides. *Protein Science* 9: 1095-1105, 2000.
 31. S Zhang, M Altman, Peptide self-assembly in functional polymer science and engineering. *Reactive and Functional Polymers* 41: 91-102, 1999.
 32. S Zhang, M Altman, Self-assembling peptide systems in biology, engineering and medicine. *Crete Meeting Proceedings (Ed. A Aggeli, N Boden, S Zhang)* Kluwer Academic Publishers, Dordrent, The Netherlands pp. 343-360. (2001)
 33. S Zhang, Emerging biological materials through molecular self-assembly *Biotechnology Advances* 20: 321-339, 2002.
 34. W Hwang, D Marini, RD Kamm, S Zhang, Supramolecular structure of helical ribbons self-assembled from a beta-sheet peptide. *J. Chem. Physics* 118: 389-397, 2003.
 35. R Ellis-Behnke, CE Semino, S Zhang, GE Schneider, Peptide nanofiber scaffold for brain lesion repair (**Submitted**), 2003.
 36. C-I Branden, J Tooze, *Introduction to Protein Structure*. 2nd Ed. Garland Publishing, New York, NY; 1999.
 37. Zhang, S. Fabrication of novel materials through molecular self-assembly. *Nature-Biotechnology* 21: 1171-1178, 2003.
 38. S Zhang, D Marini, W Hwang, S Santoso, Design nano biological materials through self-assembly of peptide & proteins. *Current opinion in Chemical Biology* 6, 865-871, 2002.
 39. S Zhang, Building from bottom-up. *Materials Today* 6: 20-27, 2003.
 40. S Santoso, S Zhang, Nanomaterials through molecular self-assembly. *Encyclopedia of Nanotechnology (In press)* 2004.

Table 5. PuraMatrix Attributes and Advantages Comparison Table

Attributes	PURAMATRIX Synthetic ECM	Natural ECM	Synthetic Scaffolds	PURAMATRIX ADVANTAGE
Scaffold Properties				Defined, consistent bare ECM analog
Composition	RAD ₁₆ 16 peptide monomer in 0.5-1.0% w/v Patented Worldwide	Collagen, Matrigel, cadaver tissue, basement membrane	PLA, PLGA, carbon fiber, calcium phosphate	Animal-free, reproducible cell culture & cell signaling
Fiber size & sequence	7-10 nm diameter Bare ECM free of unwanted signals – add components as needed	5-10 nm diameter Complex undefined protein sequences	10,000-100,000 nm looks 2D relative to cell	Approximates in vivo ECM nano-scale without the complexity
Pore size	50-400 nm	50-400 nm	20,000-1x10 ⁶ nanometers	Encapsulates like ECM
Water content	99.5-99.9%	80-97%	60-80%	Better hydration & nutrient diffusion
Mechanical strength	Low to medium, cells can migrate within it	Low to medium	Med to High	More rapid cell migration, ingrowth
Physical loading	Able to simulate physiological loading and flow	Depends on material	Often brittle, shift load from cells	Create physiologically-relevant microenviron.
Cell Encapsulation & Handling				Stable, Injectable, Customizable
Scaffold formation	Fibers and gel form around cells with simple addition of culture media or injection in vivo	Require refrigeration or complex processing	Preformed scaffolds tough to seed with cells	Superior encapsulation allows cells to create own microenvironments and surrounding ECM
Combination with bioactives	Bioactives, ECM proteins can be added for tailored reproducible 3D cultures	Inconsistent levels of proteins & GF	Yes, but not true microenvironments	Enables consistent, defined ECM microenvironments
Allows cell attachment, migration, angiogenesis	Yes, enables anchorage dependent cell culture	Yes	Some	Allows cell-cell interactions, migration and invasion assays
Sterile	Gamma irradiation or pre-gelled filter sterilization in situ	No, destroys material and proteins	No gamma, often limited to ethylene oxide	Able to use gold standard sterilization, and filter sterilize in situ if needed
Injectable	Yes, will not swell beyond injected volume. Compatible with cardiovascular catheters.	Yes, when chilled	Not injectable	Injectable along with cells, yet gel forms upon introduction in vivo
Clinical cell culture “Closed System”	Sterility (gamma irradiation) and injectability enables closed system culture for bioproduction and clinical cell expansion	Animal components discouraged by FDA	Often hard to sterilize via gamma irradiation	Gold standard sterility, combined with injectability and easy handling
Stable	Shelf stable at room temperature and across broad temperature range for at least two years.	Natural product requires refrigeration with short shelf life	Shelf stable only while dry	Ideal stability independent of water content
Molding, Coating, Sheeting	Amenable to casting, coating, layering, 3D printing	Often monolayer only or limited sheets	Fixed shapes can be cut to shape	Simple to configure as needed
Cell Recovery & Analysis				Research & clinical compatibility
Microscopy	Transparent	Often cloudy	Often opaque	Easy visualization
Cell passaging harvesting, separation	Spin cells out, wash, replate or reencapsulate	Trypsin, collagenase	Hard to harvest cells without disruption	Easy cell harvesting with high cell viability
Molecular biology	Protein monomer has simple fingerprint to distinguish	Variation & noisy background data	Not compatible	Straightforward Westerns, Southern, Northern
Flow cytometry	Compatible without separation	Must separate	Not compatible	Compatible
Closed system cell harvesting	Compatible	Depends on material	Not compatible	Requirement for clinical and bioproduction apps

Biocompatibility				Superior in vivo, Rigorously tested
Non-immunogenic	No discernable antibodies, foreign body response, chronic inflammation	More immune response and inflammation	Foreign body response, scarring, acidic breakdown	Superior in direct comparison studies
Biodegradable	Yes, rapid due to low material/water ratio	Yes, but heavy lymphocyte activity	Yes, but illicit foreign body rxn.	More rapid, but rate can be varied & controlled
Swelling/Absorption	Non-swelling upon injection	Non-swelling	Often swell, causing irritation	Consistent control of injected volume
Ingrowth, angiogenesis	Weak gel & cell migration allow rapid ingrowth	Undefined cell signaling	Large structure inhibits ingrowth	More rapid ingrowth

REFERENCES

1. J Sipe, Tissue Engineering and Reparative Medicine. *Ann. N.Y. Acad. Sci.* 961:1-9, 2002.
2. B Ratner, A Hoffman, F Schoen, J Lemons, (eds.) *Biomaterials Science*. Academic Press, New York. 1996.
3. R Lanza, R Langer, J Vacanti, *Principles of Tissue Engineering*, 2nd Academic Press, San Diego, CA. USA. 2000.
4. A Atala, R Lanza, *Methods of Tissue Engineering*. Academic Press, San Diego, CA. 2001.
5. AS Hoffman, Hydrogels for biomedical applications. *Advanced Drug Delivery Reviews*. 43: 3-12. 2002.
6. B Palsson, J Hubbell, R Plonsey, JD Bronzino, *Tissue Engineering: Principles and Applications in Engineering*. CRC Press, 2003.
7. S Ayad, RP Boot-Handford, MJ Humphreise, KE Kadler, CA Shuttleworth, *The extracellular matrix: Facts Book*. 2nd, Academic Press, San Diego, CA. 1998.
8. T Kreis, R Vale, *Guide book to the extracellular matrix, anchor, and adhesion proteins*. 2nd., Oxford University Press. Oxford, UK, 1999.
9. Yannas, I. *Tissue and Organ Regeneration in Adults*. Springer, New York, 2001.
10. DJ Mooney, LK Hansen, R Langer, JP Vacanti, DE Ingber. Extracellular matrix controls tubulin monomer levels in hepatocytes by regulating protein turnover. *Mol Biol Cell*. 5:1281-1288, 1994.
11. P Friedl, K Zanker, E Brocker, Cell migration strategies in 3-D extracellular matrix: Differences in morphology, cell matrix adhesions, and integrin function. *Microscopy Research and Technique*. 43: 369-378, 1998.
12. A Folch, M Toner, *Microengineering of Cellular Interactions*. *Ann. Rev. Biomed. Eng.* 2: 227-256, 2000.
13. B Geiger, Cell biology, Encounters in Space. *Science* 294: 1708-1712, 2001.
14. A Abbott, D Cyranoski, Biology's new dimensions. *Nature* 420: 870-872, 2003.
15. S Zhang, C Lockshin, A Herbert, E Winter, A Rich (1992) Zuotin, a putative Z-DNA binding protein in *Saccharomyces cerevisiae*. *EMBO. J*, 11: 3787-3796.
16. S Zhang, T Holmes, C Lockshin, A Rich, Spontaneous assembly of a self-complementary oligopeptide to form a stable macroscopic membrane. *Proc. Natl. Acad. Sci. USA* 90: 3334-3338, 1993.
17. S Zhang, C Lockshin, R Cook, A Rich, Unusually stable beta-sheet formation of an ionic self-complementary oligopeptide. *Biopolymers* 34: 663-672, 1994.
18. S Zhang, T Holmes, M DiPersio, RO Hynes, X Su, A Rich, Self-complementary oligopeptide matrices support mammalian cell attachment. *Biomaterials* 16: 1385-1393, 1995.
19. TC Holmes, S Delacalle, X Su, A Rich, S Zhang, Extensive neurite outgrowth and active neuronal synapses on peptide scaffolds. *Proc. Natl. Acad. Sci. USA* 97: 6728-6733, 2000.
20. J Kisiday, M Jin, B Kurz, H Hung, CE Semino, S Zhang, AJ Grodzinsky, Self-assembling peptide hydrogel fosters chondrocyte extracellular matrix production and cell division: implications for cartilage tissue repair. *Proc. Natl. Acad. Sci.*

- USA 99: 9996-10001, 2002.
21. CE Semino, JR Merok, G Crane, G Panagiotakos, S Zhang, Functional differentiation of hepatocyte-like spheroid structures from putative liver progenitor cells in three-dimensional peptide scaffolds. *Differentiation* 71: 262-270, 2003.
 22. CE Semino, J Kasahara, Y Hayashi, S Zhang, Entrapment of hippocampal neural cells in self-assembling peptide scaffold. *Tissue Engineering* 10: (**in press**) 2004.
 23. EJ León, N Verma, S Zhang, DA Lauffenburger, RD Kamm, Mechanical properties of a self-assembling oligopeptide matrix. *J. Biomaterials Science: Polymer Edition* 9: 297-312, 1998.
 24. M Caplan, P Moore, S Zhang, RD Kamm, DA Lauffenburger, Self-assembly of a beta-sheet oligopeptide is governed by electrostatic repulsion. *Biomacromolecules* 1: 627-631, 2000.
 25. M Caplan, EM Schwartzfarb, S Zhang, RD Kamm, D Lauffenburger, Control of self-assembling oligopeptide matrix formation through systematic variation of amino acid sequence. *Biomaterials* 23: 219-227, 2002.
 26. MR Caplan, EM Schwartzfarb, S Zhang, RD Kamm, DA Lauffenburger, Effects of systematic variation of amino acid sequence on the mechanical properties of a self-assembling, oligopeptide biomaterial. *J. Biomaterials Science Polymer Edition* 13: 225-236, 2002.
 27. D Marini, W Hwang, DA Lauffenburger, S Zhang, RD Kamm Left-handed helical ribbon intermediates in the self-assembly of a beta-sheet peptide. *NanoLetters* 2: 295-299, 2002.
 28. S Zhang, Design and exploitation of self-assembling ionic complementary peptide systems: A model for peptide biomaterial engineering. *Perspective in Protein Engineering 1996 (CDROM Edition)* Geisow, M. Ed. Biodigm Ltd. UK, ISBN0-9529015-0-1, 1996.
 29. Y Hong, RL Legge, S Zhang, P Chen, Effect of amino acid sequence and pH on nanofiber formation of self-assembling peptides EAK16-II and EAK16-IV. *Biomacromolecules* 4: 1433-42, 2003.
 30. M Altman, P Lee, A Rich, S Zhang, Conformational behavior of ionic self-complementary peptides. *Protein Science* 9: 1095-1105, 2000.
 31. S Zhang, M Altman, Peptide self-assembly in functional polymer science and engineering. *Reactive and Functional Polymers* 41: 91-102, 1999.
 32. S Zhang, M Altman, Self-assembling peptide systems in biology, engineering and medicine. *Crete Meeting Proceedings (Ed. A Aggeli, N Boden, S Zhang)* Kluwer Academic Publishers, Dordrent, The Netherlands pp. 343-360. (2001)
 33. S Zhang, Emerging biological materials through molecular self-assembly *Biotechnology Advances* 20: 321-339, 2002.
 34. W Hwang, D Marini, RD Kamm, S Zhang, Supramolecular structure of helical ribbons self-assembled from a beta-sheet peptide. *J. Chem. Physics* 118: 389-397, 2003.
 35. R Ellis-Behnke, CE Semino, S Zhang, GE Schneider, Peptide nanofiber scaffold for brain lesion repair (**Submitted**), 2003.
 36. C-I Branden, J Tooze, *Introduction to Protein Structure*. 2nd Ed. Garland Publishing, New York, NY; 1999.

37. Zhang, S. Fabrication of novel materials through molecular self-assembly. *Nature-Biotechnology* 21: 1171-1178, 2003.
38. S Zhang, D Marini, W Hwang, S Santoso, Design nano biological materials through self-assembly of peptide & proteins. *Current opinion in Chemical Biology* 6, 865-871, 2002.
39. S Zhang, Building from bottom-up. *Materials Today* 6: 20-27, 2003.
40. S Santoso, S Zhang, Nanomaterials through molecular self-assembly. *Encyclopedia of Nanotechnology (In press)* 2004.